

Lattice dynamics of $K_2Pt(CN)_4Br_{0.3} \cdot 3.2 D_2O$ (KCP) studied by inelastic neutron scattering

K. Carneiro* and G. Shirane

Brookhaven National Laboratory,† Upton, New York 11973

S. A. Werner† and S. Kaiser§

Scientific Research Staff, Ford Motor Company, Dearborn, Michigan 48121

(Received 17 November 1975)

The lattice-dynamical properties of the "quasi-one-dimensional conductor" $K_2Pt(CN)_4Br_{0.3} \cdot 3.2 D_2O$ (KCP) has been studied by neutron inelastic scattering at temperatures between 20 and 240 K with special attention to the relation to the partial three-dimensional ordering at $T \approx 100$ K. We have investigated the general lattice dynamics by measuring the acoustic-phonon dispersion relations. Secondly, extensive measurements have been carried out to clarify the nature of the excitations in the vicinity of the $2k_F$ anomaly, which are restricted to extremely narrow wave-vector regions. In these regions we present normalized intensity contours, which may be directly compared with theoretical calculations. At all temperatures below 160 K we find a maximum in the scattering at the $2k_F$ anomaly with an energy of 2.5 meV, as has recently been found by Comès *et al.* At lower temperatures the inelastic scattering becomes well separated in energy from the elastic scattering, signifying a phonon gap. We find it plausible to ascribe the apparent disappearance of this gap at higher temperatures to phonon lifetime effects, leading to the conclusion that the phonon frequency does not, at any temperature, condense to $\omega = 0$. At all temperatures, we find the scattering in the $2k_F$ anomaly to be connected with the regular phonons. Furthermore, the inelastic scattering intensities at the $2k_F$ anomaly is found to vary slowly with the wave-vector component perpendicular to the Pt chains and does not seem to reflect the buildup of the transverse, static correlations at lower temperatures. Our results extend previous neutron inelastic studies in several ways, and are found to be in fair agreement with the recent infrared (ir) and Raman scattering data.

I. INTRODUCTION

For the understanding of quasi-one-dimensional electrical conductors, $K_2Pt(CN)_4Br_{0.3} \cdot 3.2H_2O$ (KCP) and its deuterated counterpart has proven to be a fruitful system to study experimentally.¹ Because of the availability of good quality single crystals, this material has recently been studied by a variety of experimental techniques, providing challenging pieces of information to be compared with proposed theories. In this paper, we present inelastic neutron scattering studies of a single crystal of $K_2Pt(CN)_4Br_{0.3} \cdot 3.2D_2O$ to further illuminate the lattice-dynamical properties.

Much of the interest in KCP has been devoted to the aspects of the structural changes around $T = 100$ K. In addition to the normal Bragg reflections from the tetragonal crystal, Comès *et al.*^{2,3} discovered in an x-ray study diffuse scattering along certain reciprocal-lattice planes perpendicular to the c axis at room temperature. These scattering planes, to which we shall refer to as $2k_F$ planes are located at $Q_{\parallel} = l(2\pi/c) \pm 2k_F$, where l is an integer and k_F is the Fermi wave vector of the one-dimensional (1-D) electron gas confined to the Pt chains along the c axis. At low temperatures, the scattering in the planes sharpens around the satellite points

$$\vec{Q} = ((h + \frac{1}{2})2\pi/a, (k + \frac{1}{2})2\pi/a, l2\pi/c \pm 2k_F), \quad (1)$$

h , k , and l being integers. These authors as-

sociated the change in the x-ray scattering with the accomplishment of the Peierls transition, in which the high-temperature 1-D phase transformed into a 3-D low-temperature phase, in correspondence with the observed electronic properties.¹ Subsequent neutron scattering experiments by Renker *et al.*⁴ showed that this transition is incomplete, since long-range order perpendicular to the Pt chains never builds up. They found the linewidths of the satellites, after a rather rapid decrease as the temperature was lowered through $T = 100$ K, to saturate at a finite value. The fact that the transition is never fully accomplished remains an intriguing problem in understanding of the properties of KCP.

With improved instrumental resolution, Lynn *et al.*⁵ were able to give a detailed description of the line shapes of the elastic scattering, introducing a model for the Pt chains, in which the $Pt(CN)_4$ complexes respond as a unit in the instability. After their work the following consistent picture of the statics around the incomplete structural ordering at $T = 100$ K emerges. At all temperatures below 300 K (the crystals tend to break down at more elevated temperatures) the Pt-Pt distances in the chain are subject to a sinusoidal distortion caused by the electronic charge-density wave (CDW) formed from the Pt d_{z^2} electrons. The correlation length, ξ_{ii} , along the chain is large corresponding to more than 100 Pt-Pt distances. This sinusoidal distortion is characterized by the

wave vector $2k_F$ and the amplitude of the Pt displacement A . At high temperatures, the correlation between different chains is very weak, as described by a transverse correlation length $\xi_{\perp} = 6 \text{ \AA}$. As the temperature is lowered A and ξ_{\perp} increase, until they reach their low-temperature values of 0.025 and 80 \AA , respectively.⁶ In view of our results, as we shall discuss in Sec. V, it is interesting to notice that whereas the satellite *peak* intensities vary rapidly around $T=100 \text{ K}$, the parameters A and ξ_{\perp} , deduced from the model of Ref. 5, vary more gradually towards a saturated value at $T \approx 60 \text{ K}$. For experimental resolution reasons, only a lower limit on the parameter ξ_{\perp} has so far been set, and we have not attempted to improve this situation.

The mean positions of all the atoms in the tetragonal unit cell have been determined from crystallographic measurements.⁷⁻⁹ The structure is found to be noncentrosymmetric (space group $P4mm$). The Br^- ions appear to be randomly distributed, and perhaps also some of the water molecules; but some aspects of the positions of these two components in the unit cell are not fully resolved.

The original x-ray work^{2,3} could not resolve whether the $2k_F$ scattering was elastic, i.e., static in origin, or inelastic originating from phonons; but in a neutron scattering study, Renker *et al.*¹⁰ showed that in addition to the elastic scattering mentioned above, a contribution from a "giant Kohn anomaly" was present in the $2k_F$ scattering. However, whereas the structural aspects of KCP are at present rather well resolved, the lattice-dynamical aspects have proven more difficult to tackle. Infrared¹¹ (ir) and Raman¹² scattering experiments have measured characteristic frequencies of 2 and 5.5 meV, respectively, but the complexity of the system obscures to some extent the conclusions that can be drawn from these experiments alone. Although neutron scattering is in principle excellently suited to measure lattice dynamics, the rapid variation of the excitations around the $2k_F$ anomaly in KCP makes it impossible to measure phonon dispersions in the ordinary sense by this technique. This may indeed be the reason why two previous inelastic neutron scattering studies^{5,13} led to rather different conclusions about the excitations. In order to clarify this, we show in Fig. 1 some of the inelastic results from these papers.

Based on constant energy scans, Lynn *et al.*⁵ derived maxima in the inelastic neutron scattering, which at all temperatures above 80 K extended down to zero energy transfer. They concluded that no major changes occurred in the excitation spectrum around $T=100 \text{ K}$ at the $2k_F$ anomaly, and in the associated phonons; but they also found

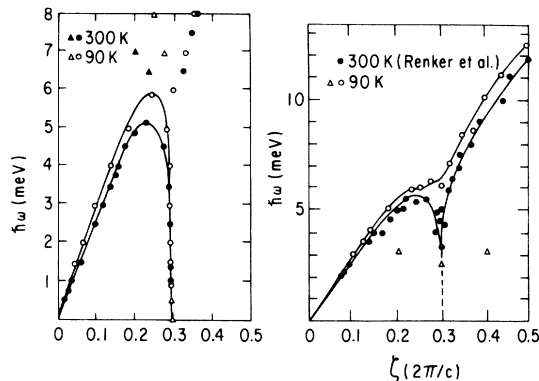


FIG. 1. Previous inelastic neutron scattering results, obtained from KCP, for phonons with propagation vector $\vec{q} = \xi \vec{c}^*$. The left-hand side shows the results of Lynn *et al.* (Ref. 5), and the right-hand side those of Comès *et al.* (Ref. 13), where the high-temperature data were taken from the original work of Renker *et al.* (Ref. 10). Circles indicate the distorted [001] LA phonon (Λ_1), and triangles show other observed maxima in the scattering. Note the different energy scales.

evidence for a *higher*-lying optical mode, the origin of which was not entirely clear. This picture is contrasted by that emerging from the work of Comès *et al.*¹³ They concluded that only at higher temperatures did the phonon soften appreciably, whereas at low temperatures the Kohn anomaly had almost disappeared. The additional scattering observed at low temperatures was then explained as a *lower*-lying optical mode.

With this discrepancy in mind, we have performed inelastic neutron scattering measurements in the temperature regime between 20 and 240 K with special emphasis below 160 K. We have measured the acoustic phonons along high-symmetry directions to explore the general lattice dynamics of KCP. Near the $2k_F$ anomaly, where the electron-phonon coupling seriously distorts the regular phonons and the wave-vector dependence is too rapid to be resolved, we have measured intensity contours of the scattering and we show how these can be compared with theoretical calculations. By analyzing our results we can explain most of the apparent differences between the previous neutron measurements, and also obtain good agreement with optical data. This together with the new results reported here extends our experimental knowledge about "quasi-one-dimensional" conductors as exemplified by KCP.

In comparing our results with ir and Raman experiments, the following is of importance. Whereas in neutron scattering, the major problem in the interpretation of the data is the wave-vector dependence of the scattering, in an optical experiment the momentum transfer is limited to essentially zero. Thus one might expect easily inter-

pretable line shapes from these experiments. However, in KCP there exist two incommensurate periodicities, one of the tetragonal unit cells (which we consider the basic), and one of the CDW. In an optical experiment one cannot determine in which of the two lattices a measured excitation occurs, i. e., one is unable to distinguish a Γ -point phonon in the tetragonal lattice from an optical excitation in the one-dimensional lattice of the CDW. In the latter case, photons will probe excitations, not at a particular point of the $2k_F$ plane, but over all of it. If therefore, the frequencies vary within these planes, the optic spectrum will be broadened, owing not only to genuine lifetimes, but also to dispersion within the $2k_F$ planes.

The paper is organized as follows. In Sec. II we describe the experimental conditions, i. e., details about the crystal and the instrumental set-up. Section III contains the measured phonon dispersion relations, and here we also derive values for the unperturbed phonon frequencies for the branches which are affected by the electron-phonon coupling. Section IV contains the scattering connected to the inelastic $2k_F$ anomaly in terms of normalized intensity contours, and the wave-vector dependence of the inelastic scattering along the $2k_F$ planes. In Sec. V we apply a simple model and discuss the values of our parameters in the context of the optical experiments and a few theoretical calculations. Our main conclusions are summarized in Sec. VI. In an appendix we describe the theory of neutron scattering, when applied to the special case of KCP.

II. EXPERIMENTAL

A. Crystal

The crystal used in our experiments was grown from solution by Ford Scientific Research Staff, yielding a 0.68-cm³ single crystal with a mosaic spread of 0.5° full width at half maximum (FWHM), and a density at room temperature of 2.729 g/cm³. The chemical unit is K₂Pt(CN)₄Br_{0.3} · 3.2(D₂O), with two such units in the tetragonal unit cell, characterized by the lattice parameters

$$a = 9.83 + 2.2 \times 10^{-4} T, \quad (2)$$

$$c = 5.69 + 2.9 \times 10^{-4} T, \quad (3)$$

where a and c are in Å and the temperature T is in K. The reciprocal-lattice unit cell is then defined by $a^* = 2\pi/a$ and $c^* = 2\pi/c$. Our values agree well with those in Ref.'s 5, 8, and 9. Also in agreement with earlier work we have found the wave vector of the CDW to be $2\vec{k}_F = 1.70 \vec{c}^*$. This implies that in reduced units the $2k_F$ planes are characterized by $q_x = 0.30 c^*$.

The crystal was encapsulated in an aluminum

container together with a small amount of D₂O to prevent loss of water. Over the two months of experiments it was kept below $T = 240$ K. We did not detect any sign of deterioration of the crystal, although we did see a small, time independent scattering at $(0, 0, 3.35)$ with an intensity of approximately 1% of the (004) diffraction peak. We have investigated this scattering, first reported by Lynn *et al.*⁵ in one of the crystals used in their experiments. This crystal, which had been temperature recycled many times and stored at room temperature, developed a very strong reflection at the above mentioned wave vector *without any noticeable change* in the characteristics of the $2k_F$ scattering. From diffraction experiments we are able to identify the formation of a layered structure, as responsible for this extra scattering.

By visual inspection of the crystal, we could see a greenish yellow phase which had grown at the expense of the copper colored normal KCP. We associate the new phase with a very dehydrated state, since dehydration normally shows up as a light yellow phase. The growth of this extra phase may be a surface effect, since it appeared mainly around grain boundaries, and on the external surface of the original crystal. As mentioned, the effect remained small during the course of the experiments reported here.

B. Instrumental

The experiments were performed at the neutron triple-axis spectrometers at the HFBR reactor at Brookhaven. In both the regular phonon measurements, and when measuring the intensity contours, several different setups were used to ensure that multiple scattering effects did not play any role. Constant- \vec{Q} scans were made with both fixed incoming neutron energy ("fixed k_i "), and with fixed outgoing neutron energy ("fixed k_f "), where in the former case, higher-order neutrons in the incoming beam were filtered out by a 2-in.-thick pyrolytic graphite filter. The monochromator and analyzer were in all cases pyrolytic graphite crystals of mosaic spread 0.4° FWHM. Further, the scans were characterized by the horizontal collimation (FWHM) of the four Soller slit collimators of the spectrometer, all with a vertical resolution of approximately 1°.

In analyzing the intensities obtained from the neutron scattering experiments, care has to be taken with respect to resolution effects, together with possible changes in the analyzer reflectivity.¹⁴ In a constant k_i scan, the integrated intensity \mathcal{I} of a narrow peak at (\vec{Q}, ω) is related to the neutron scattering law $S(\vec{Q}, \omega)$ through

$$\mathcal{I}(\vec{Q}, \omega) \sim k_f^4 \eta_A \cos \theta_A S(\vec{Q}, \omega), \quad (4)$$

where θ_A and η_A are the Bragg angle and the re-

flectivity of the analyzer. In the case of a constant k_f scan we get

$$\mathcal{T}(\vec{Q}, \omega) \sim S(\vec{Q}, \omega), \quad (5)$$

where (5) implies that a $1/v$ monitor is used in the incident beam, and data are taken at constant monitor counts. The advantage of the direct relation between the scattering law and the measured intensity in a constant k_f scan is to some extent counterbalanced by the lack of filtering of the incident beam, so we felt that both types of scans were to be used.

We have used the results (4) and (5) for the *integrated* intensities to correct our data *point by point* when appropriate, using the numerical values for the correction factors in (4) measured by Skalyo and Lurie.¹⁵ By this approximate procedure, we have made the intensity corrections to the measured scattering, but we have not corrected for the finite wave vector and energy resolution of the instrument. These latter corrections can, however, only be made when one assumes a specific form of $S(\vec{Q}, \omega)$. The normalized intensities $I(\vec{Q}, \omega)$ that we present in Sec. IV, where \vec{Q} and ω are the settings of the instrument, thus correspond to a convolution of $S(\vec{Q}, \omega)$ with a resolution function R :

$$I(\vec{Q}, \omega) = \int S(\vec{Q}', \omega') R(\vec{Q} - \vec{Q}', \omega - \omega') d\omega' d\vec{Q}', \quad (6)$$

where

$$\int R(\vec{Q}, \omega) d\vec{Q} d\omega = 1. \quad (7)$$

Because of the above intensity correction the normalization (7) is valid. Consequently (6) and (7) should be used in any detailed comparison between a theory and our experimental results, where $R(Q - Q', \omega - \omega')$ can be taken as a Gaussian distribution function.

III. PHONON DISPERSION RELATIONS

In this section we present experimental phonon dispersion relations for KCP, measured at temperatures 80, 160, and 240 K. We have not intended to give a complete picture of the general lattice dynamics, but concentrated on the acoustic phonon branches. We find that the regular phonons in KCP are anisotropic, and that the temperature dependence is not very pronounced. We also discuss why the scattering at the $2k_f$ anomaly cannot experimentally be treated as regular phonons. The more careful treatment of this is presented in Sec. IV. Figure 2 shows some of the raw data of the phonon measurements, and we associate the observed maxima in the constant- \vec{Q} scans with the phonon frequencies of the modes. Based on scans similar to those of Fig. 2 we plot in Fig. 3 the

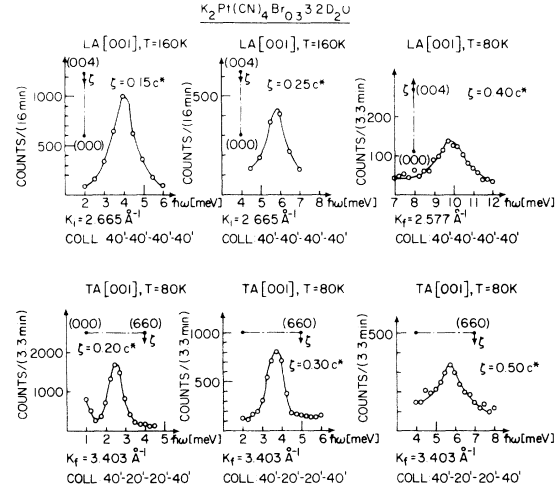


FIG. 2. Neutron groups, used to derive the phonon dispersion relations in $K_2Pt(CN)_4Br_{0.3} \cdot 3.2D_2O$, shown for the two-phonon branches propagating along the \vec{c}^* direction. The scans are characterized by the phonon propagation vector $\vec{q} = \xi \vec{c}^*$, the reciprocal lattice vector \vec{T} , and the fixed neutron wave vector (k_i or k_f). The horizontal collimation (FWHM) is shown for the four Soller slit collimators, starting with the one before the monochromator crystal.

phonon dispersion relations along high-symmetry directions. The only acoustic branch which was not measured, is the TA_{\parallel} mode propagating along the 100 direction (the Δ_2 mode).

The first thing to notice is the strong anisotropy, as seen by the much higher frequencies for the phonons having a component of propagation parallel to the c^* axis, as compared to those propagating in the basal plane of the Brillouin zone. This shows that the predominantly metallic binding along the Pt chains is strong with respect to the binding between the chains. The crystallographic structure determinations suggest the latter binding to be mainly ionic, and therefore the anisotropic elastic properties¹⁶ are not unexpected.

As mentioned above, we have not attempted a complete lattice-dynamical study, since the assignments of the optic modes would probably be extremely difficult. However, we have found some evidence for a longitudinal-optic phonon at $\hbar\omega = 6$ meV, both along Λ and V . The scattering, especially along Λ is weak, and we have so far not been able to follow this mode throughout the zones, but as we shall discuss in Sec. V, this particular phonon *might* have been observed in a recent Raman scattering experiment.¹²

The temperature dependence of the phonon spectra is on the whole rather small. This indicates that the anharmonic effects, described by phonon-phonon interactions are not very important. The main change in the frequencies seems to occur be-

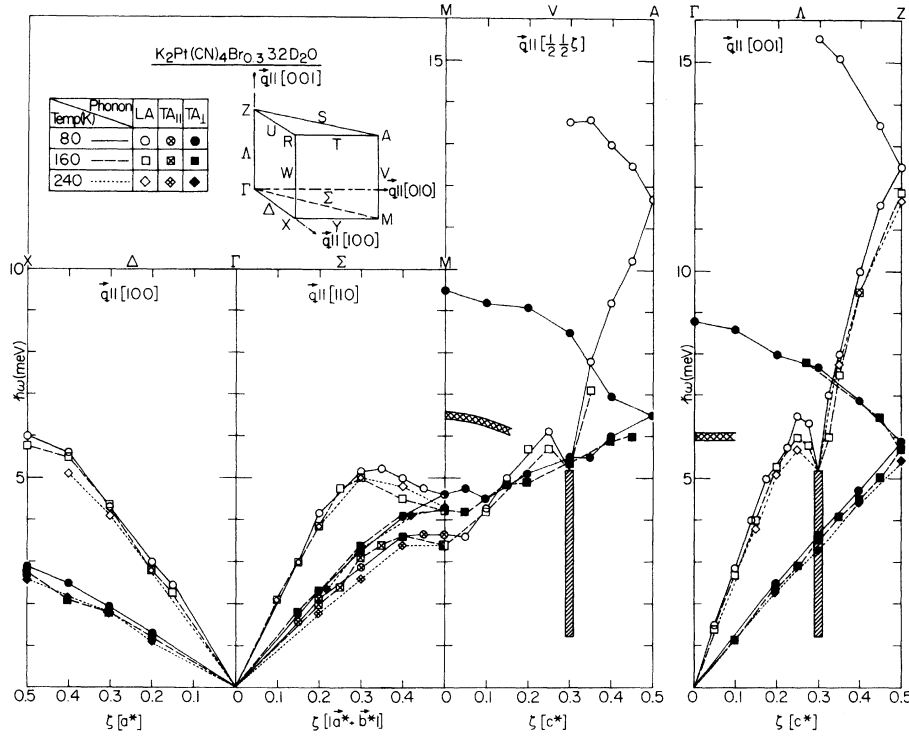


FIG. 3. Phonon dispersion relations in $K_2Pt(CN)_4Br_{0.3} \cdot 3.2O_2O$ measured at temperatures $T = 80, 160,$ and 240 K. One inset shows the assignments of the modes where \parallel and \perp refer to the polarization vector being parallel or perpendicular to the \vec{c}^* axis, respectively. The other inset shows the irreducible part of the Brillouin zone. The lines are intended only to connect the data points. The shaded areas correspond to $q_x = 2k_F$, where the wave-vector dependence of the scattering cannot be resolved. The cross-hatched areas show the position of the weak scattering that may correspond to an optic phonon.

tween 80 and 160 K, where the incomplete structural ordering takes place. If phonon-phonon interactions were dominant one would expect the temperature dependence to progress with increasing temperature.

We now focus our attention on the two phonon branches which show the $2k_F$ anomaly, indicated as shaded areas in Fig. 3. In Fig. 4 we replot the experimental results, the $[001]LA$ (Λ_1) phonon branch on the left-hand side, and on the right-hand side the corresponding phonon with propagation vector $\vec{q} = (\frac{1}{2}, \frac{1}{2}, \zeta)$, the V_1 mode. First we try to identify the unperturbed phonon frequency $\omega_0(\vec{q})$ which is of interest for the theoretical discussion of the electron-phonon coupling. If we assume only nearest-neighbor interactions, and recall that there are two $Pt(CN)_4$ groups per unit cell, we get for the $[001]LA$ branch

$$\omega_0(\zeta) = \omega_{\max} \sin(\frac{1}{2}\pi\zeta), \quad (8)$$

where ω_{\max} is the maximum value of the unperturbed phonon. This maximum frequency does not appear at the zone boundary but is reflected into the zone center, since we measure ζ in units of $c^* = 2\pi/c$, corresponding to the full unit cell. The solid line in Fig. 4 represents such a dispersion relation drawn through the points away from the $2k_F$ anomaly at $T = 80$ K. Since we get good agreement on both sides of $\zeta = 0.3$, we believe this procedure to give a reliable $\omega_0(\vec{q})$, yielding in par-

ticular $\omega_0(0, 0, 0.30) = 8.1$ meV. Similarly we derive for the right-hand side of this figure the bare phonon frequencies, and find $\omega_0(\frac{1}{2}, \frac{1}{2}, 0.30) = 8.0$ meV. The procedure applied here to find the unperturbed phonon frequency seems to work satisfactorily. An alternative procedure would be to measure phonons at very high temperatures, where the Kohn anomaly had disappeared. This is not feasible, in part because of the crystal deterioration at high temperature.

The observed frequencies $\omega(\zeta)$ in Fig. 4 show the following features. For $\zeta = 0.3$ the phonons are softened with a temperature dependence, which is most pronounced between $T = 80$ and 160 K. Although not displayed, at $T = 160$ and 240 K, we find evidence of finite lifetimes for $\zeta \geq 0.2$ (measured with an energy resolution of approximately 1 meV). The temperature dependence of $\omega(\vec{q})$ and the lifetimes of the modes appear to be similar along Λ and V . Although $\omega_0(\vec{q})$ is different in the two cases, the renormalization $\omega_0(\vec{q}) - \omega(\vec{q})$ seems to differ little. At $\zeta = 0.30$ on both sides of Fig. 4, the constant- \vec{Q} scans show an extra maximum at $\hbar\omega = 2.5$ meV at the temperatures 80 and 160 K. This peak was observed by Comès *et al.*¹³ at the lower temperature. We ascribe it to better experimental circumstances that we are able to see it also at $T = 160$ K. However, in contrast to our findings, they found the maximum to extend over an appreciable wave-vector region, as shown on the right-

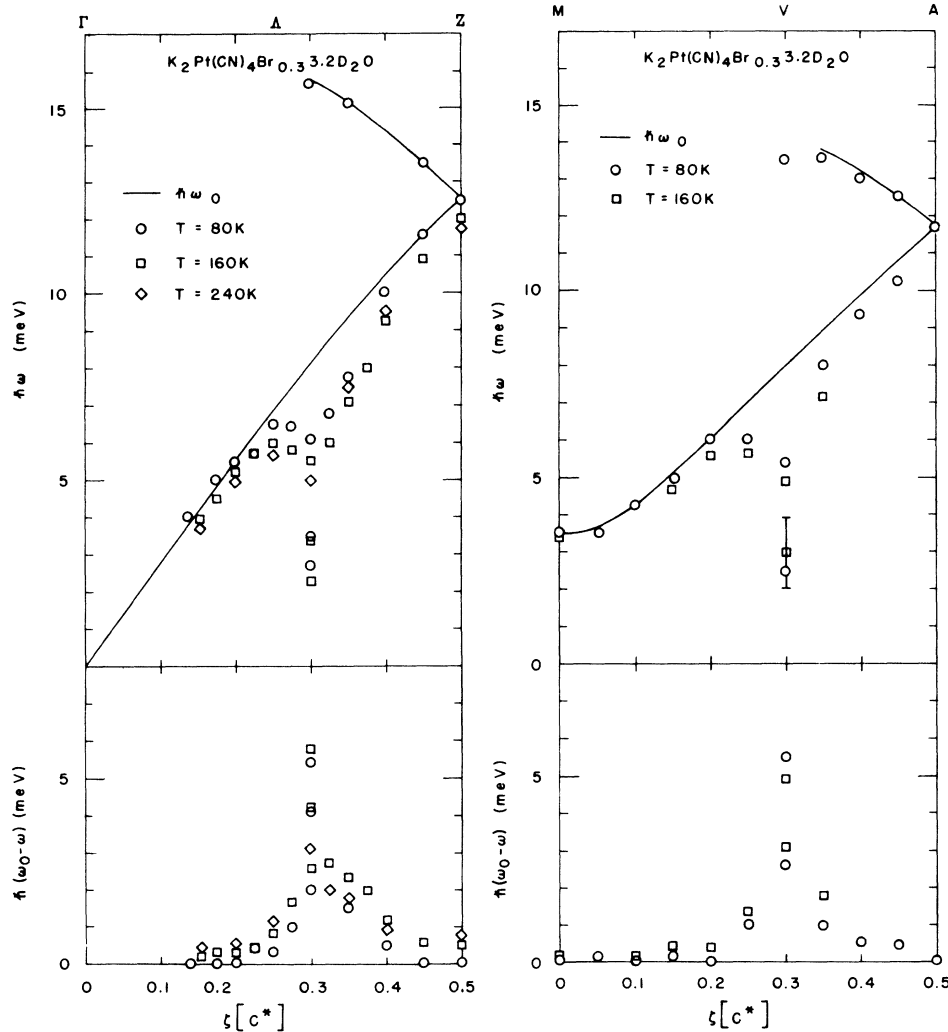


FIG. 4. Maxima observed in constant- Q scans. The left-hand side shows the [001] LA phonon branch with propagation vector $\vec{q} = (0, 0, \zeta)$ (Λ_1), and the right-hand side shows that propagating with $\vec{q} = (\frac{1}{2}, \frac{1}{2}, \zeta)$ (V_1). The solid line corresponds to the estimated unperturbed phonon frequency $\omega_0(\zeta)$, derived as described in the text. The bottom part shows the renormalization $\omega_0(\zeta) - \omega(\zeta)$.

hand side of Fig. 1 by the triangles at $\zeta = 0.2$ and at 0.4 . This led them to ascribe the scattering at energies of 2.5 meV to the existence of a low-lying optic mode. We observe the 2.5 -meV maximum only at $\zeta = 0.30$, giving rise to the following problem. Since at $\zeta = 0.30$, we see more than one maximum in the scattering from a constant- \vec{Q} scan, but only one at other wave vectors, we cannot unambiguously combine points of maxima in the ω - q plane to form a dispersion curve for the excitations. This problem arises because we are unable to resolve the wave-vector dependence of the $2k_F$ scattering. In this case neutron scattering is unable to reveal the excitation spectrum with the certainty that usually characterizes this method, when applied to lattice dynamics. We shall, therefore, in Sec. IV, present the measured intensities instead of only the observed maxima. This provides better insight into the nature of the excitations, and a better testground for comparison with theoretical calculations.

IV. INTENSITY MEASUREMENTS

We have measured the neutron scattering intensities in the vicinity of the $2k_F$ anomaly, for the phonons propagating with $\vec{q} = (0, 0, \zeta)$, i. e., along the Λ line in the Brillouin zone, and $\vec{q} = (\frac{1}{2}, \frac{1}{2}, \zeta)$, i. e., along the V line. We have normalized the intensity using the prescription outlined in Sec. III. In the first case data were taken at nine different temperatures below 240 K, whereas in the latter case the measurements were performed at fewer temperatures. All the data presented in this section were taken in the region of reciprocal space with Q_x between 3.5 and 4.0 , and $Q_x (= Q_y)$ between 0 and 0.5 . Typical raw data are shown in Fig. 5. A combination of constant- \vec{Q} scans and constant E scans was used to reveal the characteristics of the scattering. In order to deduce the coherent part of the scattering one has to subtract incoherent-elastic as well as incoherent-inelastic scattering, together with "real" background not originating

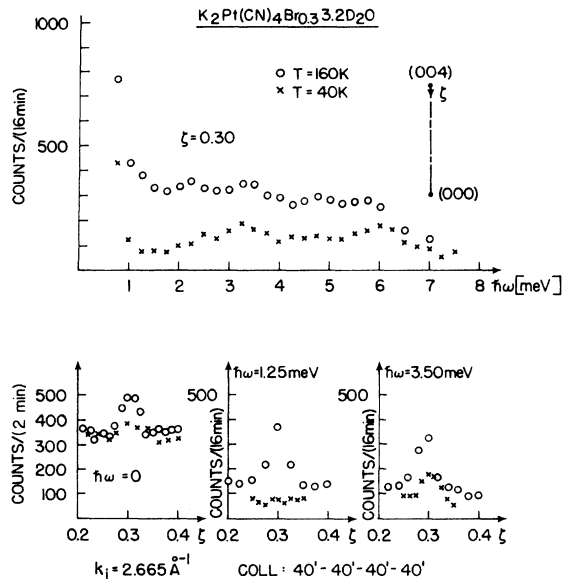


FIG. 5. Raw data, used in the measurements of the neutron scattering intensity contours for $K_2Pt(CN)_4Br_{0.3} \cdot 3.2D_2O$, shown for the excitations of wave vector $\vec{q} = \zeta\vec{c}^*$. The upper part shows a constant- Q scan at $Q_x = 2k_F$, and the bottom part shows some constant- E scans across the $2k_F$ anomaly.

from the sample. As explained in more detail in the Appendix the elastic-incoherent scattering can be identified as the ζ -independent part of the elastic scattering. Subtracting this, we get the remaining coherent elastic scattering at $\zeta = 0.30$. The inelastic background (incoherent and "real" background) was taken to be the slowly varying scattering away from the regular phonon and the $2k_F$ scattering. Having subtracted these contributions, we associated the remaining scattering with $S(\vec{Q}, \omega)$ and corrected it as described in Sec. III, yielding the normalized scattering $I(\vec{Q}, \omega)$ to be interpreted according to (6) and (7).

In Figs. 6–8 we present the contours of constant scattering based on the measured $I(\vec{Q}, \omega)$, shown for selected temperatures. As support for the description of these figures, we show in Fig. 9 some constant- Q scans at $Q_x = 3.70$, which as we shall see, contains all the information gained about the excitations at energies below 4.5 meV, when the temperature is kept below 160 K. The primary reason for producing Figs. 6–9 is that the normalized intensities may be quantitatively compared with any theoretical calculations of $S(\vec{Q}, \omega)$, when folded appropriately with the instrumental resolution (shown in each figure) according to (6) and (7). Although the ultimate understanding of the nature of the excitations is of course obtained via a theory that fits the data, we shall in the following characterize the results on purely experimental

grounds. By this we hope to give an unbiased presentation of the results, thereby setting some criteria, which any successful theory must satisfy.

The intensity in the $2k_F$ anomaly appears always to be connected continuously to the regular phonon branches. At energies less than 4.5 meV no resolvable wave-vector widths are observed at temperatures below 160 K. At $T \geq 80$ K the scattering also extends down to $\omega = 0$, however with a pronounced saddlepoint at $\hbar\omega \approx 1.25$ meV at 80 K, showing that a constant- E scan (horizontal in the figures) would give a maximum at $\zeta = 0.3$, whereas a constant- Q scan (vertical in the figures) would give a minimum. At 80 K the connection to the regular phonons also goes through a saddle point at $\hbar\omega \approx 4.5$ meV, although less pronounced than the lower one.

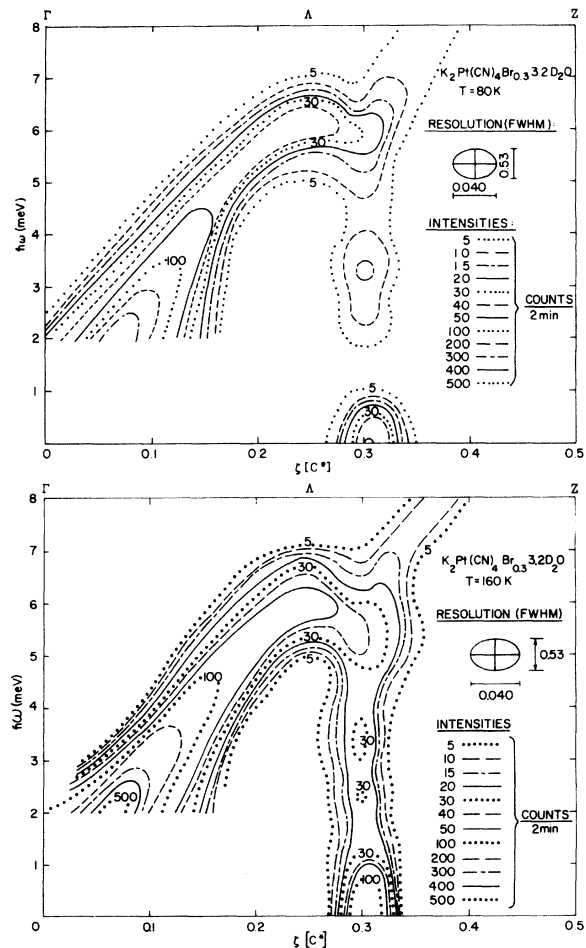


FIG. 6. Normalized intensity contours of the neutron scattering from the excitations of wave vector $\vec{q} = \zeta\vec{c}^*$ at $T = 80$ and 160 K, measured with an average resolution as indicated. The elastic incoherent scattering and the inelastic background has been subtracted. The intensity unit counts/(2 min) is not to be taken as representative of the actual counting time.

Since lifetime effects might smear out the observed peaks, one cannot easily resolve whether the dispersion relations for the excitations are connected through the saddlepoints of the scattering. However our data at lower temperatures reveal the following. Below $T=60$ K we see zero inelastic scattering in the region below $\hbar\omega = 1.75$ meV. This is illustrated at $T=40$ K in Fig. 5, where a constant- E scan at $\hbar\omega = 1.25$ meV did not show a maximum. In the corrected intensities from a constant- Q scan at $\zeta=0.3$, as shown in Fig. 9, this is seen as zero scattering at lower energies, separable from the resolution extended elastic scattering. This feature, signifying the existence of a phonon gap, is most clearly found at $\vec{q}=(0,0,0.30)$. Here, the elastic scattering is relatively small compared to that at $\vec{q}=(\frac{1}{2}, \frac{1}{2}, 0.30)$ where it extends rather far out in energy, at low

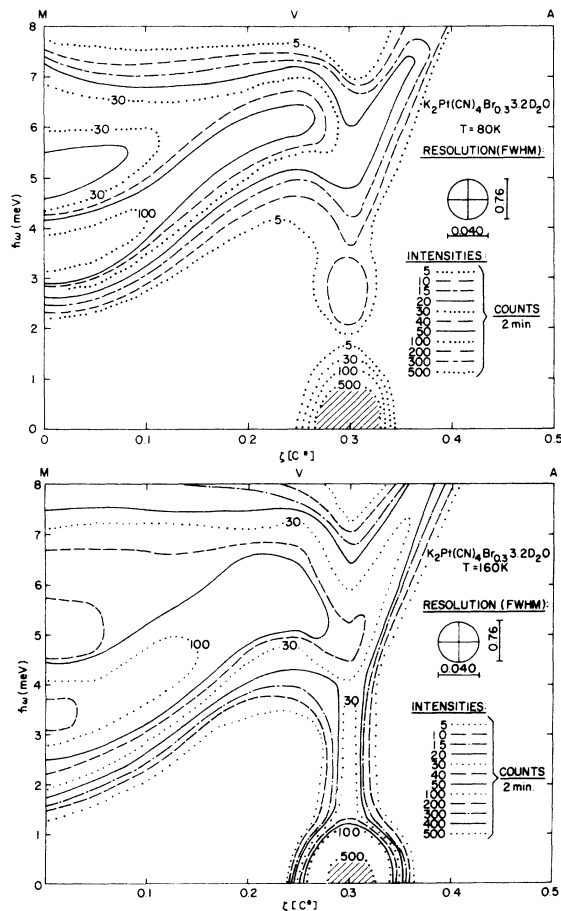


FIG. 7. Normalized intensity contours of the neutron scattering from the excitations of wave vector $\vec{q}=(\frac{1}{2}, \frac{1}{2}, \zeta)$ at $T=80$ and 160 K, measured with an average resolution as indicated. The elastic incoherent scattering and the inelastic background has been subtracted. The intensity unit counts/(2 min) is not to be taken as representative of the actual counting time.

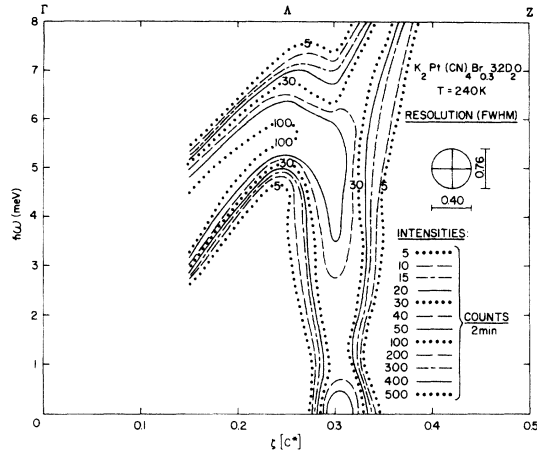


FIG. 8. Normalized intensity contours of the neutron scattering from the excitations of wave vector $\vec{q}=\zeta\vec{c}^*$ at $T=240$ K, measured with an average resolution as indicated. The elastic incoherent scattering and the inelastic background has been subtracted. The intensity unit counts/(2 min) is not to be taken as representative of the actual counting time.

temperatures, as seen in the intensity contours.

The scattering at the saddle point at $\hbar\omega \approx 4.5$ meV does not go to zero as the temperature is lowered to 20 K, but seems to saturate at 60 K. In contrast to the results of Ref. 13 (of Fig. 1), we do not find any wave-vector extension of the scattering in $2k_F$ anomaly below 4.5 meV. Thus we are led to the conclusion that the excitations responsible for this scattering are at all tempera-

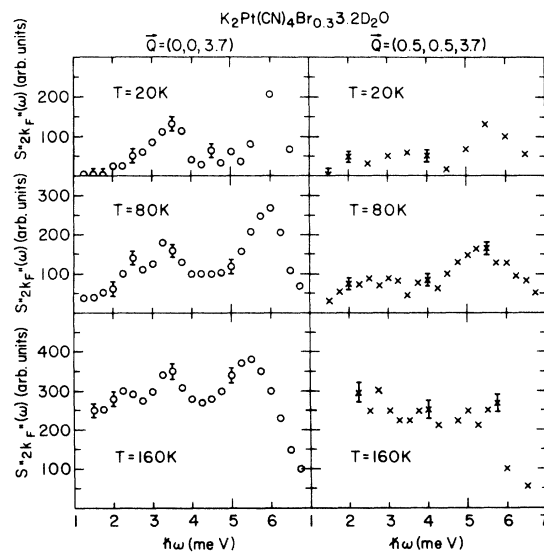


FIG. 9. Normalized inelastic scattering at the $2k_F$ anomaly at $\vec{Q}=(0,0,3.70)$ and at $\vec{Q}=(\frac{1}{2}, \frac{1}{2}, 3.70)$ shown at different temperatures. Note the offset of the energy axis.

tures connected to the regular phonons.

The existence of an apparent phonon gap for temperatures less than 60 K at $\zeta=0.3$ is a new experimental finding. The reason why this feature was not found in previous studies is probably that they were done with smaller crystals, so that the inelastic scattering could not be extensively investigated below $T=80$ K. However, with this new result in mind it still remains an important question whether the extension of the scattering at higher temperatures down to $\omega=0$ is due to a softening of ω ($\zeta=0.30$), the phonon frequency at the $2k_F$ plane, or is due to an increased damping. In order to illuminate this, we focus on the following. At temperatures less than 160 K as seen in Figs. 6, 7, and 9 we always observe a maximum at $\hbar\omega \approx 2.5$ meV, which naturally is associated with the structure in the scattering around ω ($\zeta=0.30$). Also if this frequency was decreased, the scattering would increase dramatically because of the ω^{-1} term in the one-phonon cross section (see Appendix) and not show the saddle point observed around $\hbar\omega=1.25$ meV. We find it therefore most natural to conclude that ω ($\zeta=0.30$) does not condense to zero for any temperature, but rather stays at a finite value of $\hbar\omega \approx 2.5$ meV, with lifetimes responsible for the change in the scattering. The rather structureless scattering in the contour diagram obtained at $T=240$ K, shown in Fig. 8, can be understood as resulting from very short lifetimes at this temperature.

In all the intensity contours we also find a maximum in the scattering at $\zeta=0.3$ and $\hbar\omega \approx 6.0$ meV. Since the scattering around this peak shows finite wave-vector dependence it is tempting to associate the points of maxima with a well-defined dispersion relation, thus implying the existence of two modes at $\zeta=0.3$. This is certainly possible. However, as we shall discuss in Sec. V, one may with certain assumptions reproduce all the scattering by assuming that only one branch exists. But we disagree with the conclusion of Ref. 13 that only one branch exists at high temperatures whereas two are present at $T=80$ K.

As mentioned above, Lynn *et al.* reported an extra mode, lying above the regular phonon branch at wave vectors $\zeta < 0.3$. From Figs. 6 and 8 it is evident that a maxima will occur in a constant E scan due to the finite energy width of the phonon, at wave vectors $0.25 \leq \zeta < 0.3$, in addition to the maximum coming from the dispersion relation at $\zeta \leq 0.3$. Thus we conclude that the extra points of maxima, do not represent the dispersion relation for a separate excitation.

Although we are able to explain most of the differences in the conclusions in Refs. 5 and 13, concerning the phonon spectrum around the $2k_F$ anomaly, we are left with two pieces of information,

complicating the interpretation of our data. One originates from the scattering probably coming from an optic phonon of energy 6 meV, as shown in Fig. 3 (horizontal cross-hatched regions). This frequency was not observable at the (004) Γ point, which corresponds to $\zeta=0$ in the diagrams in Figs. 6 and 8, but only around (003). However, it was clearly significant at the $(\frac{1}{2}, \frac{1}{2}, 4)$ M point, as seen in Fig. 7, and here it appears as flowing into the phonon associated with the $2k_F$ anomaly. This may be a combination of resolution and varying phonon structure factor, and we find it unlikely that this mode influences the character of the $2k_F$ scattering. We would like to point out that although we cannot at the present assign conclusively a particular motion to this optic frequency, the intensity as described here, follows what one would expect if the mode originated from the two $\text{Pt}(\text{CN})_4$ complexes in the unit cell, moving with opposite phases.

Another feature in the inelastic intensities, is the appearance of a third peak at $\vec{q}=(0, 0, 0.30)$ which is not seen at $\vec{q}=(\frac{1}{2}, \frac{1}{2}, 0.30)$. This peak at $\hbar\omega=3.5$ meV appears in the contour diagrams of Fig. 6, and also in the left-hand side of Fig. 9. At first sight it seems to obstruct the picture of the scattering in $2k_F$ anomaly as being essentially independent of \vec{Q}_1 . There are various possible origins of this peak. Since we find it in several scattering geometries, it is unlikely to come from multiple scattering. One could suspect that it is an artifact from the finite instrumental resolution, giving rise to an instrumental coupling to the transverse phonon in a nominally longitudinal scan. Then, however, the scattering would be unlikely to peak in a narrow wavevector region as we see it in Fig. 6. Also, this interpretation is inconsistent with the fact that we do not see the extra peak in Fig. 8. The enhanced scattering observed at $\zeta=0.30$ with $q_1=0$ occurs where the transverse acoustic branch crosses the longitudinal $2k_F$ excitations, and consequently points towards a real coupling between the two. We shall discuss this in more detail in the next section, and here only mention another experimental observation regarding this problem. One might expect that the observed increase in the intensity at $\hbar\omega=3.5$ meV in the "longitudinal" branch should be reflected in a change of the intensity from the "transverse" branch. Without being conclusive, we do observe a small decrease in transverse intensity at $q=(0, 0, 0.30)$, in support of our interpretation. It should of course be kept in mind that the reason why this coupling is not observed when $\vec{q}=(\frac{1}{2}, \frac{1}{2}, 0.30)$ is that the transverse mode crosses the longitudinal just above the $2k_F$ anomaly as seen in Fig. 3.

In order further to illuminate the nature of the

scattering, we have complemented the contour diagrams with intensity measurements in the $2k_F$ planes as a function of $\vec{q}_\perp = (\zeta, \xi, 0)$. In Fig. 10 we show the intensities for the energies 0, 2.5, and 3.5 meV for the temperatures 80, 160, and 240 K. The inelastic scattering varies rather little with \vec{q}_\perp and the temperature, as opposed to the elastic scattering where the perpendicular correlations strongly enhance the scattering at $\xi=0.5$, at lower temperatures. This shows that the lower-lying excitations in the $2k_F$ anomaly are at all temperatures weakly correlated perpendicular to the Pt chains, consistent with a small dispersion perpendicular to the c axis. The similarity between the low-energy inelastic data, and the high-temperature elastic data, as seen in Fig. 10, suggests that the inelastic scattering follows the structure

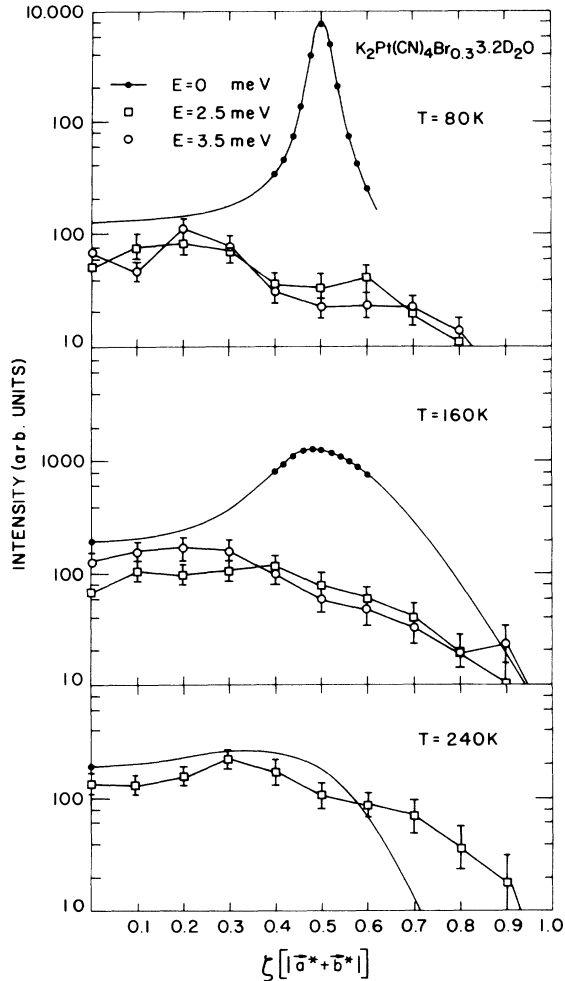


FIG. 10. Variation of the normalized intensity in the $[110]$ direction of a $2k_F$ plane, shown at temperatures $T=80, 160,$ and 240 K. The solid line is calculated from the model of Lynn *et al.* Note that at all temperatures, the inelastic scattering resembles the elastic at high temperatures.

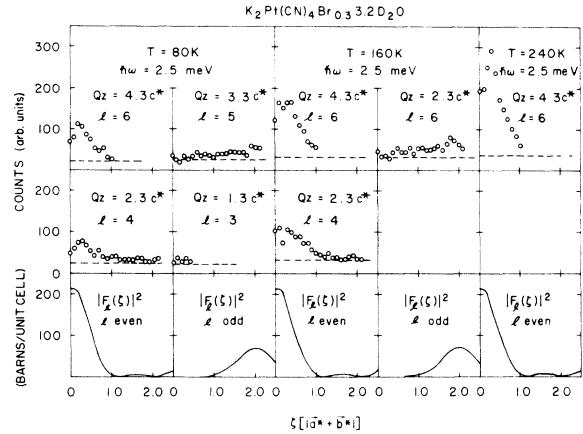


FIG. 11. Variation of the inelastic intensity ($\hbar\omega=2.5$ meV) in the $[110]$ direction of several $2k_F$ planes, shown for $T=80, 160,$ and 240 K, compared with the structure factor $F_1(\zeta)$, calculated by Lynn *et al.*

factor $F_1(\zeta)$ calculated by Lynn *et al.* This is further illustrated in Fig. 11, where we have measured the $\hbar\omega=2.5$ meV scattering in several different $2k_F$ planes. The apparent agreement between $|F_1(\zeta)|^2$ and our measurements is a strong indication that, as one might anticipate, only the motion of the $Pt(CN)_4$ complexes is responsible for the scattering at $\vec{q}_\perp=0.30\vec{c}^*$. We find it rather unlikely that an optic mode, as discussed in Ref. 13, would exhibit this characteristic dependence perpendicular to \vec{c}^* .

V. DISCUSSION

After having presented our data without assuming any form of the excitation spectrum in Sec. IV, we shall now give a more specific discussion based on particular model for the dispersion for the excitations in the $2k_F$ anomaly. In doing so, we shall point out that, although the recent ir and Raman experiments could be successfully interpreted within the framework of a one-dimensional pinned CDW model, our results cannot be consistently analyzed via this model. However, by comparing directly our results and the optical observations we find good agreement.

In Sec. IV we found that at energies $\hbar\omega \leq 4.5$ meV we could not resolve any intrinsic wave-vector width of the scattering in the $2k_F$ anomaly and that the inelastic scattering was weakly dependent on q_\perp . Let us therefore consider a model for the excitations that only includes the dependence on q_x . We neglect at first the variation of the one-phonon structure factor $F(Q)$ [we set $F(Q)=1$], especially that related to the coupling between the nominally longitudinal and transverse phonon branches at $q_\perp=0$. The model is shown in Fig. 12. It has a linear part of slope v , not necessari-

ly pointing towards $q'_z=0$, where q'_z measures q_z with respect to a $2k_F$ plane. This linearly sloping phonon is cut off by a flat part of frequency ω_T , which extends over a region ΔQ . We consider a finite lifetime Γ for the flat part, but not in the sloping regime. (The scattering would only depend weakly on a finite lifetime in the sloping region.) The qualitative form of the scattered intensity is also shown in Fig. 12. Taking into account that the instrumental wave-vector resolution is wider than the distance AB in Fig. 12, one sees that the spectrometer integrates over q'_z . We show in the Appendix that the scattering from the sloping regime becomes

$$S_{2k_F}(\omega) = [n(\omega) + 1] / \omega v. \quad (9)$$

Similarly, we get from the flat part

$$S_{2k_F}(\omega) = [n(\omega) + 1] \frac{1}{\pi} \frac{4|\omega|\Gamma\Delta Q}{(\omega^2 - \omega_T^2)^2 + 4\omega^2\Gamma^2}. \quad (10)$$

By fitting the expressions (9) and (10) to the observed scattering at a series of temperatures below 160 K, we get the results as shown in Fig. 13. For $\hbar\omega \leq 2.5$ meV we interpret the energy dependence of the scattering according to (10) which determines both ω_T and Γ . Since ΔQ in (10) and v^{-1} in (9) appear as multiplying factors, an absolute measurement of these quantities would re-

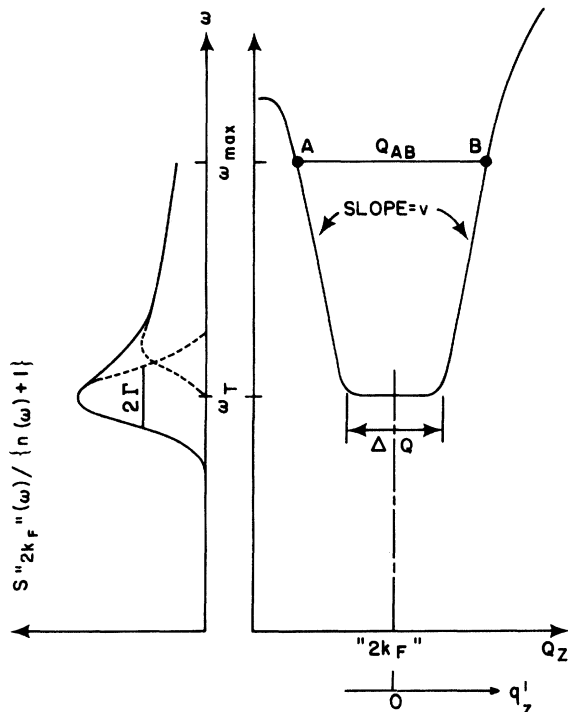


FIG. 12. Model for the excitation spectrum in the $2k_F$ anomaly, used to analyze the neutron scattering intensities below $\hbar\omega = 4.25$ meV. The left-hand side shows the expected neutron line shape.

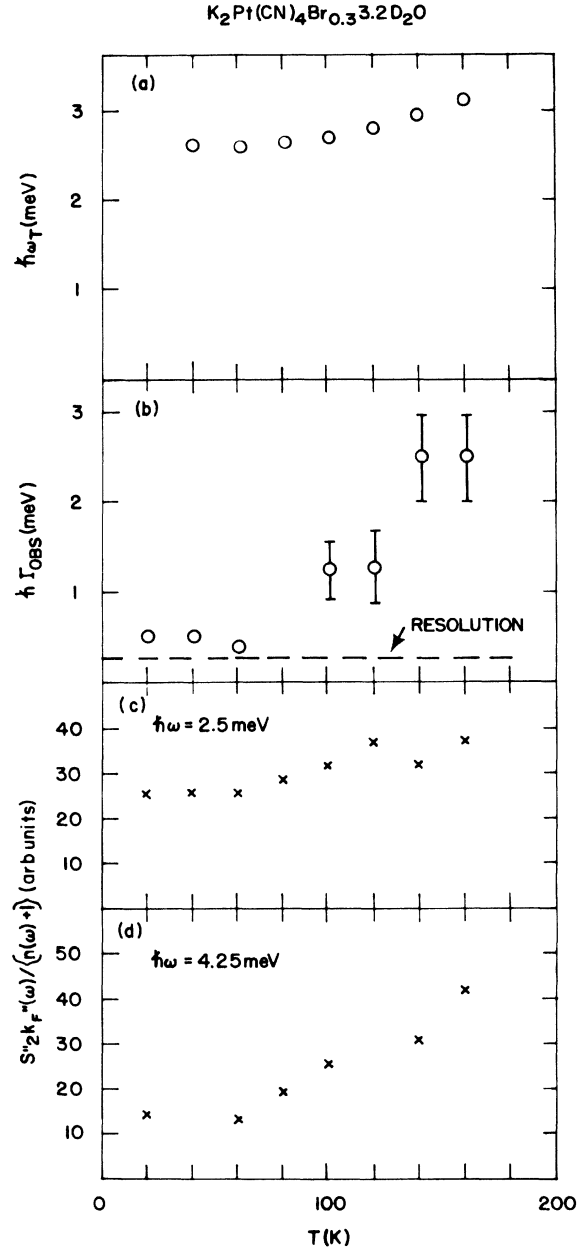


FIG. 13. Data interpreted according to the model discussed in Sec. V, shown in Fig. 12. (a) and (b) show the parameters ω_T and Γ , respectively, (c) gives ΔQ (when ω_T and Γ are determined), and (d) determines v . The values found for ΔQ and v are shown in Table I.

quire an absolute measurement of intensity. However, their ratio is determined from our relative intensity data. In order to estimate ΔQ and v on an absolute scale we make use of the fact that the distance AB in Fig. 12 is less than our resolution, setting an upper limit on AB of half our wave-vector resolution at all temperatures. Since both v^{-1} and ΔQ are largest at $T = 160$ K, the results at

TABLE I. Values for the parameters ΔQ (upper limits) and v (lower limits) for the model of the excitation spectrum in the $2k_F$ anomaly in KCP. Note that the free-electron Fermi velocity is $v_F = 11 \times 10^5$ m/sec.

Temp (K)	20	40	60	80	100	120	140	160
ΔQ (\AA^{-1})	0.002	0.002	0.002	0.003	0.005	0.006	0.010	0.011
v (10^5 m/sec)	2.0	2.0	2.0	1.5	1.1	1.0	0.9	0.7

this temperature determine the scale; that is, by setting the upper limit on AB at the highest temperature, and studying the temperature dependence of the intensities, we obtain a much smaller limit on AB at the lower temperatures. In comparing intensities to (9) and (10) we have tried to avoid frequencies, where the finite curvature between the flat and the sloping part, as drawn in Fig. 12, would be of importance. With this in mind, we have determined ΔQ from (10), using the scattering at $\hbar\omega = 2.5$ meV [shown in Fig. 13(c)], and v from (9) using the scattering at $\hbar\omega = 4.25$ meV [shown in Fig. 13(d)].

By this procedure, in addition of ω_T and Γ , displayed in Fig. 13, we obtain lower limits for v and corresponding upper limits for ΔQ shown in Table I, giving the following picture of the excitations at the $2k_F$ anomaly. At temperatures below 60 K, we get $\hbar\omega_T = 2.6$ meV, $\hbar\Gamma = 0.4$ meV, and $v \geq 2.0 \times 10^5$ m/sec. At higher temperatures Γ increases gradually as v decreases. The cut off frequency ω_T shows a slight increase with temperature, which in fact depends on the assumed form of the damping, as reflected in (10). We always get a value for ΔQ so that the relation $\omega = vq'_x$ for $\omega > \omega_T$ is satisfactorily obeyed. We find it interesting to notice that although the inelastic data, as presented in Fig. 10, did not seem to reflect the structural ordering at $T = 100$ K, our parameters v , ΔQ , and Γ do indeed vary in much the same way as the static parameters A and ξ_1 (called Γ in Ref. 5). All these parameters seem to vary gradually with temperature down to 60 K, where they obtain their low-temperature saturation values.

The simple model described above, explains successfully the inelastic scattering at the $2k_F$ anomaly at energies below 4.5 meV, except the maximum at 3.5 meV, seen at the spectrometer setting $q_1 = 0$, i.e., along the Λ line in the Brillouin zone. As mentioned in Sec. IV, we ascribe this extra intensity to a coupling between the longitudinal and transverse branches, which cross where the enhanced "longitudinal" scattering is observed. As mentioned, we also find some evidence of a corresponding decrease in the "transverse" scattering. Within the space group $P4mm$ the mixing between the two modes is not allowed on the Λ

line, and we have not been able to identify the incommensurate distortion as responsible for breaking this symmetry property. Thus the two branches must cross without interference or change in polarization vectors, as shown in the left-hand part of Fig. 14. However, the spectrometer will, at the setting $q_1 = 0$, probe excitation slightly away from its nominal value. But as soon as the wave-vector is pointing infinitesimally away from the Λ line, the two branches in question are not allowed to cross, giving rise to the picture at the right-hand side of Fig. 14, showing two repelling modes. We find it quite likely that although the $2k_F$ scattering strictly speaking then occurs in two different branches, it does not change its characteristic polarization. This implies that the polarization vectors of the branches will change as a result of the symmetry-required repelling. Taking our wave-vector resolution into account we expect this mixing of the "longitudinal" and "transverse" branches to show up only as a change in the observed intensities at the resolution broadened "crossing" point. We find that this feature deserves considerably more experimental as well as theoretical attention than outlined here.

For the scattering at the $2k_F$ anomaly at ener-

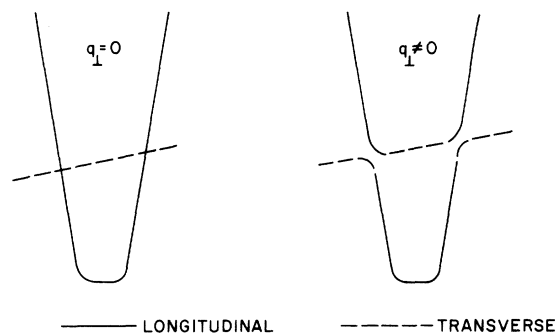


FIG. 14. Qualitative picture of the region, where a transverse phonon branch crosses the longitudinal. On the c^* axis where $q_1 = 0$, symmetry requires the two branches to cross without interacting, as shown in the left-hand side. At any general point in the Brillouin zone the picture is however that of the right-hand side, where the two branches repel each other. As discussed in the text, we suggest that the polarizations of the two branches change when they interact.

gies higher than 4.5 meV, a peak at 6 meV (see Fig. 9) appears well resolved both in energy and wave vector, indicating the existence of a higher-lying separate mode. This was indeed concluded by Comès *et al.* from their low-temperature neutron scattering results,¹³ and also by Steigmeier *et al.* from Raman scattering.¹² However, this feature in the neutron scattering may also be explained as coming from the lower-energy mode, modelled above, extending to higher energies with a sudden decrease in the velocity, so that the scattering according to (9) will give the maximum.

Lee, Rice, and Anderson¹⁷ have considered theoretically the excitations for a CDW below a Peierls transition. In the purely one-dimensional case, the transition occurs at $T=0$, but owing to finite 3-D correlations, the transition temperature becomes finite. It must however be emphasized that their theory applies only below this transition where 3-D long-range order is present, and it remains a question whether such a theory is relevant in the case of KCP, where the range of order perpendicular to the 1-D electron gas never exceeds eight chain distances. Based on the recent low-temperature ir and Raman experiments, one might conclude that this theory has been experimentally verified. Assuming the theory to be correct, we should associate our low-lying mode with the phason excitations of the CDW. Using our low-temperature data, we get for the effective electronic mass with respect to the free-electron value

$$m^*/m = (v_F/v)^2 \lesssim 30, \quad (11)$$

where v_F is the free-electron Fermi velocity.

Second, associating the loci of maxima at $\hbar\omega = 6$ meV with the amplitude excitation $\omega_+(q'_x)$ of CDW, and also analyzing the curvature of this mode around its minimum value at $q'_x = 0$ we get

$$\lambda = [\omega_+(0)/\omega_0(0)]^2 = 0.56 \quad (12)$$

and

$$m^*/m = \frac{3}{4}(v_F q'_x)^2 / [\omega_+^2(q'_x) - \omega_+^2(0)] \approx 5000, \quad (13)$$

where λ is the electron-phonon coupling and $\omega_0(0)$ is the unperturbed phonon frequency (8.1 meV) given in Sec. III. Also according to the theory the following relation holds:

$$m^*/m = 1 + 4\Delta^2 / [\lambda\omega_0^2(0)], \quad (14)$$

where 2Δ is the electronic energy gap. Using the above value for λ and taking $\Delta = 100$ meV from the ir measurements, we get $m^*/m = 1.1 \times 10^3$ in fair agreement with (13), but not comparable with (11). The different values for m^* derived from (11) and (13) reflect the experimental finding that the proposed phason mode is very steep, whereas the amplitude mode appears well resolved. In the

theory the dispersions of the two modes are restricted to be almost the same, in disagreement with our result.

In the absence of the 3-D coupling, the Peierls transition would occur at $T=0$. Horowitz *et al.*¹⁸ have considered the phonons in this case and found several similarities with the results of Ref. 17. Since the transition in KCP is never fully accomplished this approach seems conceptually more satisfactory, and we find it of interest that in the latter calculation the dispersion of the two excitations considered in Ref. 17 differ considerably, in agreement with our experimental results. The two theories, however, have in common that the electron-phonon coupling, as determined by (12) was anticipated to be approximately half the value we find.

These two theories both picture the transition in an oversimplified way with respect to KCP, either as well defined at a finite temperature in the 3-D case, or at $T=0$ in the 1-D case. Sham and Patton¹⁹ have given a model describing the partial structural ordering observed in KCP, with impurities responsible for the lack of long-range order, even at $T=0$. Quantitatively they do not however reproduce the large value for $\xi_{||}$ inferred from experiments. For the excitations, they get one mode, the "giant Kohn anomaly" exhibiting an impurity induced phonon gap. The numerical calculations, regarding the dynamical properties in their theory, have however not been published.

Returning now to the dispersion perpendicular to \vec{c}^* , we concluded from the intensity measurements that ω_T did not depend strongly upon q_1 . Although at $\vec{q}_1 = (\frac{1}{2}, \frac{1}{2}, 0)$ we cannot measure ω_T accurately, because of the strong elastic scattering, it appears from Fig. 9 that a decrease in ω_T of about 0.5 meV at this wave vector with respect of $q_1 = 0$ is in agreement with our data. The numerical values for ω_T were derived at $q_1 = 0$. In the case of the maximum at $\hbar\omega = 6$ meV at $q_1 = 0$ (at low temperatures) we find a decrease of 0.5 meV, when measured at $\vec{q}_1 = (\frac{1}{2}, \frac{1}{2}, 0)$ and here we can also resolve a significant decrease with increasing temperature. As discussed above, we attribute the extra peak at $\hbar\omega = 3.5$ meV at $q_1 = 0$ to a coupling to the transverse mode. Thus we expect this feature to be reproduced by a theory, only if it includes a calculation of the eigenvectors.

Our disagreement with the theory of Ref. 17 is not related to differences between our results and what has been found by the ir and Raman experiments. Rather, our disagreement with the theory originates from our measurements away from $q'_x = 0$. Also the conclusions about the optic work were based mainly on symmetry properties of the excitations, which one might expect to be the same for temperatures above a transition. When we

compare our experimentally observed frequencies with the ones measured by optic means, we obtained as discussed below, satisfactory agreement.

Brüesch *et al.*¹¹ found a resonance at $\hbar\omega = 1.9$ meV ($=15$ cm⁻¹) from ir reflectivity measurements obtained with a rather big uncertainty. Our values of $\hbar\omega = 2.5$ meV therefore agree reasonably well, but in the interpretation of the optic measurements, it was not considered that ω_T could vary along the $2k_F$ plane. As pointed out in Sec. I, photons will probe excitations in the $2k_F$ anomaly of wave vectors $q'_z = 0$, and cannot distinguish between different perpendicular wave-vector components. Thus in the ir spectrum a broadening will occur owing to the dependence of ω_T on q_\perp . However, we get $\hbar\Gamma = 0.4$ meV at $T = 60$ K in agreement with the ir measurements, indicating that ω_T does not vary much along the $2k_F$ planes. Our model parameters consequently correspond well with the ir data with regard to both ω_T and Γ below $T = 160$ K. At higher temperatures both their spectra and ours are broad, so we have refrained from fitting our data to a model of the kind discussed here.

To compare our data with the recent Raman scattering data reported by Steigmeier *et al.*¹² meets another complication. They observed a mode at $\hbar\omega \approx 5$ meV, which agrees fairly well with both our weak optic mode at $q = 0$ (Γ point) as well as the maximum that we observe at the $2k_F$ anomaly. If we assume however, in accordance with the authors, that the Raman scattering comes from the $q'_z = 0$ mode, it has to be interpreted similarly to the ir measurements, which also in this case improve the agreement between the two experiments at low temperatures. But at higher temperatures the two measurements yield significantly different results, so that at $T = 240$ K we measure the peak at $\hbar\omega \leq 5.2$ meV as opposed to the Raman value of $\hbar\omega \approx 6$ meV. In this case the maximum is still well defined at the highest temperatures.

VI. CONCLUSIONS

Our inelastic neutron scattering measurements on a single crystal of $K_2Pt(CN)_4Br_{0.3} \cdot 3.2D_2O$ have given the following main results.

The acoustic and related phonon branches have been measured at temperatures $T = 80, 160,$ and 240 K. They show an anisotropy reflecting that the metallic binding along the Pt chains is strong compared to the ionic binding perpendicular to them. The temperature dependence is found to be rather small. Only the longitudinal phonons propagating along the chains are found to be significantly distorted into the $2k_F$ anomaly, and in this case we derived values for the unperturbed phonons.

The inelastic scattering in the $2k_F$ anomaly shows an apparent phonon gap below $T = 60$ K,

whereas at all temperatures the scattering is connected continuously to the regular phonons. In analyzing the inelastic line shapes, we are led to the conclusion that the phonon frequency never goes to zero; and we then ascribe the observed low-energy scattering to lifetime effects at higher temperatures. At temperatures $T \leq 160$ K the wave-vector dependence of the scattering below $\hbar\omega = 4.5$ meV cannot be resolved, whereas at $T = 240$ K the effect of finite wave-vector width is seen. The scattering displayed as constant intensity contours provide a convenient test ground for theory.

By assuming a specific form of the excitation spectrum around the $2k_F$ anomaly, we can parameterize our results and compare to theoretical calculations. Owing to the narrowness of the observed spectrum we are unable to give a quantitatively consistent interpretation of the excitations, as coming from a charge-density wave below a Peierls transition. Our results do however agree satisfactorily with experimental results, obtained from infrared and Raman scattering, which were successfully interpreted within this picture, and we find that the optic data can equally well be interpreted without assuming that the transition has taken place. In taking the composite experimental evidence into account we consequently conclude that in KCP, the transition is never fully accomplished.

At all temperatures we find relatively little variation of the inelastic intensities in the $2k_F$ anomaly with respect to the propagation vector component perpendicular to the Pt chains. It is similar to the elastic scattering at higher temperatures, but does not seem to reflect the incomplete structural ordering occurring around $T = 100$ K. However, the dynamical parameters derived from our model, vary similarly to the static parameters, obtained from the elastic measurements.

At present, there exist several conflicting theories of KCP, all explaining some features of the observed properties correctly. It is our hope that the experimental evidence presented here, will be helpful in clarifying the physics responsible for the behavior of this material, towards a more unified and rigorous understanding.

ACKNOWLEDGMENTS

We have profited greatly from discussions with many of our colleagues. Especially we want to thank J. D. Axe, R. Comès, V. J. Emery, J. W. Lynn, B. R. Patton, and L. J. Sham.

APPENDIX

We present here the theory for the interpretation of the neutron scattering as appropriate for the

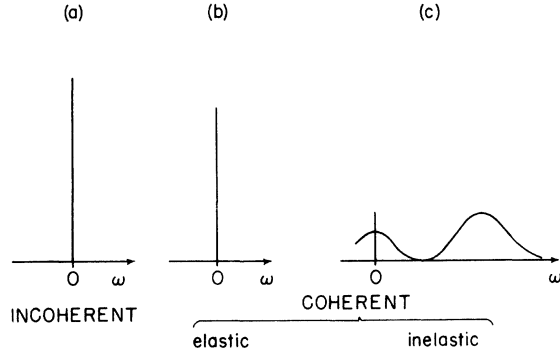


FIG. 15. Components of the neutron scattering spectrum from KCP at a $2k_F$ plane. (a) Incoherent elastic scattering present at all wave vectors. (b) Coherent elastic scattering present only at the $2k_F$ plane. (c) Inelastic coherent scattering from lattice excitations. The incoherent inelastic scattering appears as a smooth background.

lattice dynamics of KCP. Let us first assume a harmonic lattice and consider the coherent one-phonon creation scattering law $S(\vec{Q}, \omega)$,²⁰

$$S(\vec{Q}, \omega) = \frac{n(\omega) + 1}{\omega} |F(\vec{Q})|^2 \sum_{\vec{q}} \delta(\omega - \omega_0(\vec{q})) \delta(\vec{Q} - \vec{\tau} \pm \vec{q}), \quad (\text{A1})$$

where

$$\hbar \vec{Q} = \hbar(\vec{k}_f - \vec{k}_i) \quad (\text{A2})$$

and

$$\hbar \omega = (\hbar^2/2m_n)(k_f^2 - k_i^2) \quad (\text{A3})$$

are the momentum and energy, transferred to the sample by a neutron. The incoming and outgoing wave vectors are \vec{k}_i and \vec{k}_f , respectively. Since we consider only phonon creation (neutron energy loss), in (A1) $n(\omega) = [\exp(\hbar\omega/k_B T) - 1]^{-1}$ is the Bose population factor. The unperturbed phonon frequency is $\omega_0(\vec{q})$, and $\vec{\tau}$ is a lattice vector. $F(\vec{Q})$ is the inelastic structure factor, expressed in terms of the eigenvectors together with the masses, positions, and Debye-Waller factors of the atoms in the unit cell.

If the phonons cannot be regarded as free quasiparticles, due to either phonon-phonon or phonon-electron interactions, the formula (A1) must be modified. These effects can be taken in account if we replace the δ function $\delta(\omega - \omega_0(q))$ in (A1) by

$$\frac{1}{\pi} \frac{4\omega^2 \Gamma(\vec{q})}{[\omega^2 - \omega_0^2(\vec{q})]^2 + 4\omega^2 \Gamma^2(\vec{q})}. \quad (\text{A4})$$

We are therefore describing the interactions in terms of a renormalized phonon frequency $\omega(\vec{q})$ and a damping $\Gamma(\vec{q})$. Although (A4) represents a simple approach to quasiparticle interactions, we have not pursued the interpretation of our data beyond it, despite the fact that for systems exhibiting

soft-mode behavior above a structural phase transition one often needs to consider the explicit frequency dependence of Γ . This creates, under certain circumstances, a quasielastic central peak in the one-phonon scattering law, in addition to damped propagating modes.²¹

There are two reasons for confining our discussions to this simple picture. First, we find that (A4) substituted into (A1) adequately describes our observations away from the quasielastic region, suggesting the sufficiency of our treatment. Second, we are experimentally prevented from observing the central peak which we illustrate in Fig. 15. Because the soft phonon appears at $Q_x = 2k_F$ we are observing two rather strong elastic contributions to the scattering, namely the inevitable incoherent scattering [Fig. 15(a)] together with the elastic coherent scattering [Fig. 15(b)]. These two contributions, broadened by the instrumental resolution will overshadow a possible quasielastic part of the one-phonon scattering [Fig. 15(c)].

Since, at the $2k_F$ anomaly the wave-vector variation in the z direction of the lower-energy part of $S(\vec{Q}, \omega)$ is so rapid, we cannot resolve it experimentally. We therefore consider the form of the scattering, when $S(\vec{Q}, \omega)$ is integrated over Q_x in the vicinity of a $2k_F$ plane, that is, we define

$$S_{2k_F}(\omega) = \int dQ_x S(\vec{Q}, \omega), \quad (\text{A5})$$

where $\vec{Q} = \vec{Q}_x + \vec{Q}_z$, and the integration is performed over a region of Q_x much wider than the width $2k_F$ anomaly.

Two simple types of excitations are of interest for the interpretation of our data in Sec. VI. Neglecting for simplicity \vec{Q}_z , let us first consider an undamped branch of slope v :

$$\omega(Q_x) = v(Q_x - Q_0), \quad \Gamma = 0, \quad (\text{A6})$$

where Q_0 is not necessarily chosen so that the dispersion curve goes through $\omega = 0$ at a $2k_F$ plane. This inserted into (A1) and (A5) yields

$$S_{2k_F}(\omega) = |F(Q)|^2 [n(\omega) + 1] (\omega v)^{-1}, \quad (\text{A7})$$

independent of Q_0 . Next, we consider the case of a flat branch with constant damping, extending over a region ΔQ :

$$\omega(q'_z) = \omega_T \quad \text{and} \quad \Gamma(q'_z) = \Gamma \quad \text{for} \quad |q'_z| \leq \frac{1}{2} \Delta Q, \quad (\text{A8})$$

where we have defined the propagation vector q'_z with respect to the $2k_F$ planes (see Fig. 12). In this case we get

$$S_{2k_F}(\omega) = |F(\vec{Q})|^2 [n(\omega) + 1] \times \frac{1}{\pi} \frac{4|\omega| \Gamma \Delta Q}{(\omega - \omega_T)^2 + 4\omega^2 \Gamma^2}. \quad (\text{A9})$$

(A7) and (A9) show that if one assumes a certain

form of the excitation spectrum, the scattering observed according to (A5) will contain directly

interpretable information about the parameters of the modes, responsible for the scattering.

*Present address: Physics Laboratory I, University of Copenhagen, Denmark.

†Work performed under the auspices of the U. S. Energy Research and Development Administration.

‡Present address: Physics Dept., University of Missouri, Columbia, MO. 65201.

§Present address: Chemistry Dept., Massachusetts Institute of Technology, Cambridge, Mass. 02139.

¹See, for example, *One-Dimensional Conductors*, edited by H. G. Schuster (Springer, Berlin, 1975), where most of the work up to 1974 is covered.

²R. Comès, M. Lambert, and H. R. Zeller, *Phys. Status Solidi B* **58**, 587 (1973).

³R. Comès, M. Lambert, H. Launois, and H. R. Zeller, *Phys. Rev. B* **8**, 571 (1973).

⁴B. Renker, L. Pintschovius, W. Gläser, H. Rietschel, R. Comès, L. Liebert, and W. Drexel, *Phys. Rev. Lett.* **32**, 836 (1974).

⁵J. W. Lynn, M. Iizumi, G. Shirane, S. A. Werner, and R. B. Saillant, *Phys. Rev. B* **12**, 1154 (1975).

⁶C. F. Eagen, S. A. Werner, and R. B. Saillant, *Phys. Rev. B* **12**, 2036 (1975).

⁷C. Peters and C. F. Eagen, *Phys. Rev. Lett.* **34**, 1132 (1975).

⁸G. Heger, B. Renker, H. J. Dieseroth, H. Schultz, and G. Schreiber, *Mater. Res. Bull.* **10**, 217 (1975).

⁹J. M. Williams, F. K. Ross, M. Iwata, J. L. Petersen, S. W. Peterson, S. C. Lin, and K. Keefer, *Solid State Commun.* **17**, 45 (1975).

¹⁰B. Renker, H. Rietsch, L. Pintschovius, W. Gläser, P. Brüesch, D. Kuse, and M. J. Rice, *Phys. Rev. Lett.* **30**, 1144 (1973).

¹¹P. Brüesch, S. Strässler, and H. R. Zeller, *Phys. Rev. B* **12**, 219 (1975).

¹²E. F. Steigmeier, R. Loudon, G. Harbeke, H. Auderset, and G. Schreiber, *Solid State Commun.* **17**, 1447 (1975). Results obtained from a deuterated sample differ somewhat from the values reported from the hydrogenated sample [E. F. Steigmeier (private communication)].

¹³R. Comès, B. Renker, L. Pintschovius, R. Currat, W. Gläser, and G. Schreiber, *Phys. Status Solidi B* **71**, 171 (1975).

¹⁴G. Dolling and V. F. Sears, *Nucl. Instrum. Methods* **106**, 419 (1973).

¹⁵J. Skalyo, Jr., and N. A. Lurie, *Nucl. Instrum. Methods* **112**, 571 (1973).

¹⁶We do not consider the data presented in this paper appropriate for deriving accurate elastic constants of KCP. We shall present those in a later paper.

¹⁷P. A. Lee, T. M. Rice, and P. W. Anderson, *Solid State Commun.* **14**, 703 (1974).

¹⁸B. Horowitz, M. Wegner, and H. Gutfreund, *Phys. Rev. B* **9**, 1246 (1974).

¹⁹L. J. Sham and B. R. Patton, Ref. 1 p. 272.

²⁰*Thermal Neutron Scattering*, edited by P. A. Egelstaff (Academic, 1965), p. 28.

²¹The applicability of this form for the interpretation of neutron scattering results, has been discussed by J. D. Axe, G. Shirane, S. M. Shapiro, and T. Riste, in *Anharmonic Lattices, Structural Transitions, and Melting*, edited by T. Riste (Noordhof, Leiden, 1974), p. 23.